Journal of Alloys and Compounds 517 (2012) 87–91

Contents lists available at SciVerse ScienceDirect

Journal of Alloys and Compounds

journal homepage: www.elsevier.com/locate/jallcom

Magneto-electric properties of Nd substituted $BiFeO_3$ polycrystalline samples

Ashish Gautam [a,*], K. Singh [a], K. Sen [a], R.K. Kotnala [b], M. Singh [a]

[a] Material Science Laboratory, Department of Physics, Himachal Pradesh University, Shimla 171005, India
[b] National Physical Laboratory, New Delhi 110012, India

ARTICLE INFO

Article history:
Received 9 July 2011
Received in revised form 3 December 2011
Accepted 11 December 2011
Available online 24 December 2011

Keywords:
Data storage materials
Dielectric response
Phase transitions
Calorimetry
Magnetic measurements
Scanning electron microscopy (SEM)

ABSTRACT

In the present work we are reporting the dielectric properties of the samples having chemical composition $Bi_{1-x}Nd_xFeO_3$ ($x = 0, 0.05, 0.10, 0.15$), prepared by the solution combustion technique. The SEM investigation has suggested that the Nd substitution hinders the grain growth. In dielectric measurements it has been found that Nd substitution significantly improved the dielectric behaviour of the compound. Temperature dependence of dielectric constant showed the signs of magneto-electric coupling in the samples. The anti-ferromagnetic to paramagnetic transition temperature (T_N) obtained by M–T and DSC measurements was found to be in good agreement with the temperature response of dielectric constant. The ac conductivity of the samples has been found to decrease with increasing Nd content, which is desirable from the technological point of view.

1. Introduction

In the world of digital signals ferromagnetic and ferroelectric materials are being used in every aspect of science and technology. The thrust of miniaturization of devices and high density power efficient data storage systems has directed the research to a family of materials called "*Multiferroic materials*". Multiferroic, materials are the technologically important material exhibiting two or more primary ferroic orderings simultaneously viz. ferroelectric, ferromagnetic, ferroelastic, and recently proposed ferrotoroidic. Multiferroics, simultaneously having ferromagnetic and ferroelectric ordering could be used in place of their parent ferroelectric and ferromagnetic materials and with such type of materials, one can think of a new set of devices having increased efficiency and performance [1]. There are only a few known multiferroic materials which have been found because, ferroelectricity and ferromagnetism (antiferromagnetism) tend to be mutually exclusive [2]. Among the few room temperature single-phase multiferroics reported so far [3], $BiFeO_3$ shows the highest ferroelectric polarization, with a ferroelectric Curie temperature (T_C) of ~830 °C and an antiferromagnetic (AFM) Néel temperature (T_N) of ~370 °C. The ferroelectric mechanism in BFO is conditioned by the stereo-chemically active $6s^2$ lone pair of Bi^{3+}, while the weak ferromagnetic property is caused by residual moment from the canted Fe^{3+} spin structure. The coupling effect between magnetic and electric behaviours occurs through the lattice distortion of BFO when an electric field or a magnetic field is applied. Both ferroelectricity and antiferromagnetism have been known in $BiFeO_3$ single crystals [4–6], and recent studies of $BiFeO_3$ thin films [7–12] have confirmed the existence of a large ferroelectric polarization, as well as a small magnetization, both of which are consistent with theoretical predictions [13,14].

Numerous studies have been performed on $BiFeO_3$ samples and especially more recently on thin films. The structure and properties of the bulk single crystal form have been extensively studied. But, there are still some difficulties which have limited its development like; it is hard to get single phase compound with high electrical resistivity and ferromagnetism [15]. It has been found that the magnetism and ferroelectricity in BFO can be improved by substituting A-site ion with rare-earth [15–18] or alkaline-earth [19,20] ions or replacing B-site ion with transition-metal and rare-earth ones [21–24].

In our previous work [16], we have focused on structural and magnetic properties of $Bi_{1-x}Nd_xFeO_3$ and found that Nd substitution has helped in attaining the single phase and also improved the magnetism of the system. In the present work we are reporting the dielectric study of the same system.

2. Experimental procedure

The samples with chemical composition of $Bi_{1-x}Nd_xFeO_3$ say $BNFO_x$ (where $x = 0$, 0.05, 0.10, 0.15) were synthesised by solution combustion technique. The precursor was prepared in 2-methoxy ethanol taking metal nitrates and L-alanine (fuel) in stoichiometric proportions. During synthesis, an excess of 5 wt% Bi was added to the solution to compensate some unavoidable bismuth oxide loss during the

* Corresponding author. Tel.: +91 0177 2830950; fax: +91 0177 2830775.
E-mail addresses: a.matphys@gmail.com, ashishgautam2583@gmail.com (A. Gautam).

0925-8388/$ – see front matter © 2011 Elsevier B.V. All rights reserved.
doi:10.1016/j.jallcom.2011.12.025

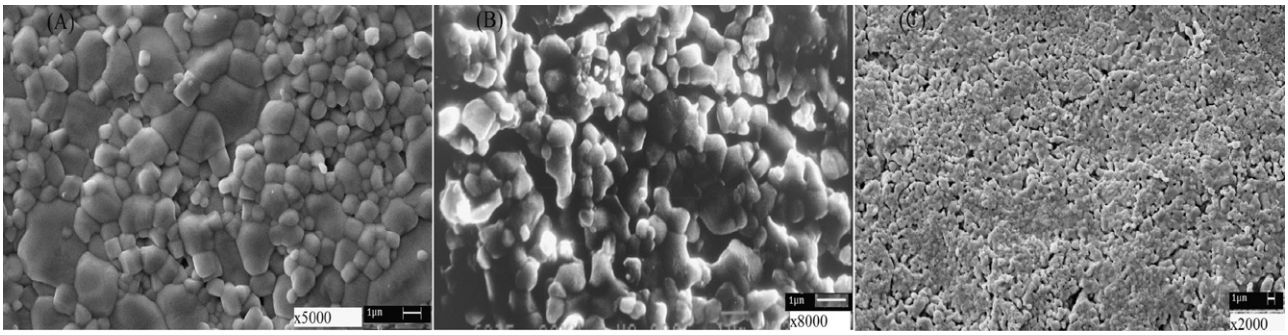

Fig. 1. (A–C) SEM images of $BNFO_x$ (x = 0.05, 0.10 and 0.15) respectively; showing the variation of grain size with Nd substitution.

thermal treatment. The solution was heated on a hot plate with continuous stirring. After heating for about half hour auto combustion was started and this process last only for few seconds. A fluffy brown mass was remained in the container. The obtained powder was calcined at 400 °C for 2 h to remove remaining organic compounds and at 850 °C for 30 min to get desired crystalline phase. The powder was then pressed to form pellets for dielectric measurements, the polyvinyl alcohol was used as binder. The pellets were finally calcined at 850 °C for 30 min and after that, silver contacts has been made on the both the flat surfaces. The microstructure of the fractured surface was observed using scanning electron microscope (SEM). The differential scanning calorimetric studies were performed on Linseis DSC system. The dielectric measurements were performed with Wayne kerr 6500B impedance analyzer in frequency range 100 Hz to 1 MHz. The magnetic measurement was carried out using a Lakeshore 7400 series vibrating sample magnetometer (VSM).

3. Results and discussion

The Rietveld crystal structure refinement of X-ray diffraction data has suggested the structural change with Nd substitution from rhombohedral ($R3c$) to triclinic ($P1$) [16]. The cell volume has been found to vary from 372.597 Å^3 for $Nd_{0.0}$ to 356.2977 Å^3 for $Nd_{0.15}$ due to smaller size of Nd ion. The SEM investigation has been performed on fractured surface of the $BNFO_x$ (x = 0.05, 0.1, 0.15) pellets sintered at 850 °C/30 min. The heterogeneous microstructure with grain size distribution has been observed, consisting from large grains with equivalent average size of ~3 μm and small grains of 300 nm (Fig. 1). The grain size is found to decrease with the increase in Nd content in the $BNFO_x$ system. The decrease in grain size may be attributed to the difference in the ionic radius of Bi^{3+} (117 pm) and Nd^{3+} (112.3 pm) and variation in bond strength which is almost twice for Nd—O bond in comparison to the Bi—O bond. These reasons are responsible for the difference between lattice constants of $BiFeO_3$ and $NdFeO_3$, and furthermore, to the difference in melting point and crystallisation temperature.

The FTIR spectra of powders $BNFO_x$ (x = 0, 0.05, 0.10, 0.15) were recorded (Fig. 2). Typical band characteristics of oxygen–metal bonds were observed in the region around 600 cm^{-1}. Independently of Neodymium content, the samples are almost free of carbonates. This result is satisfactory from a technological point of view since; presence of carbonates could result in porous pellets due to their elimination during the sintering process of the pellets. The O—H bond stretching near 3400 cm^{-1} could be attributed to adsorbed water due to the contact of the sample with the environment.

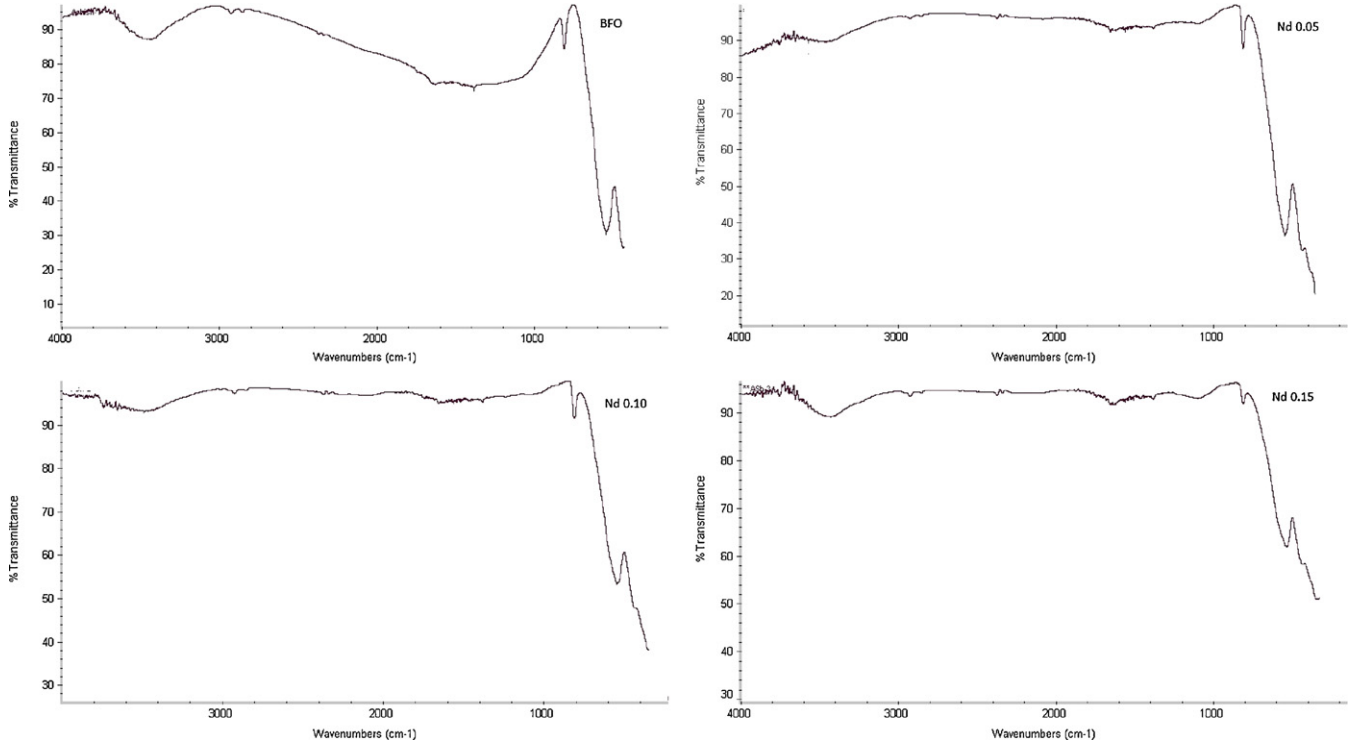

Fig. 2. FTIR spectra of $BNFO_x$ (x = 0, 0.05, 0.10 and 0.15).

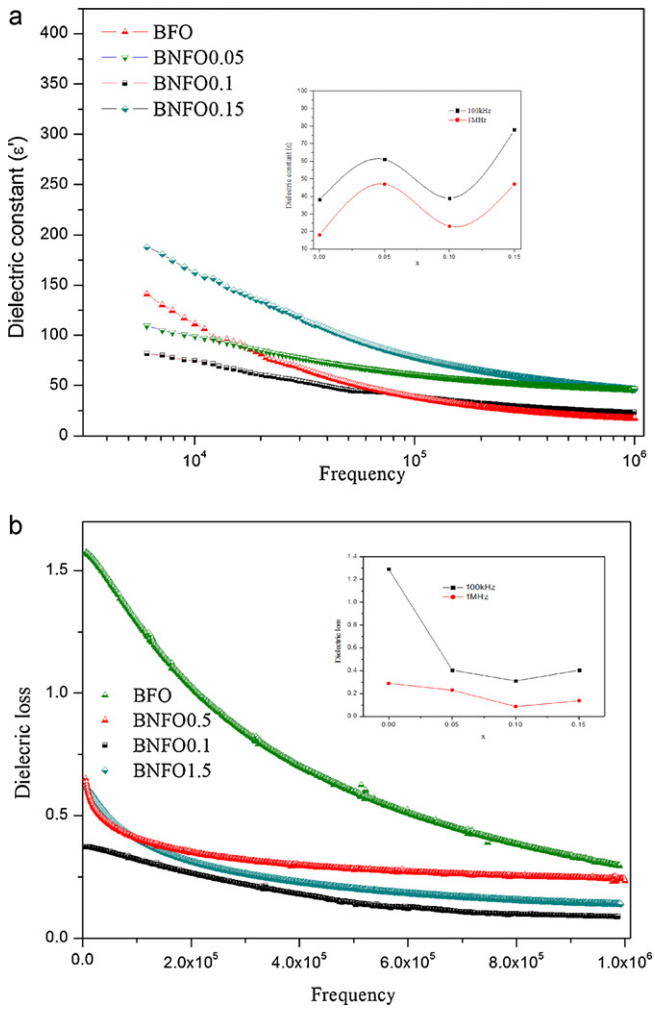

Fig. 3. (a) The variation of dielectric constant (ε_r) with frequency; in inset value of dielectric constant is plotted as a function of Nd content. (b) The variation of dielectric loss ($\tan\delta$) with frequency; inset shows the effect of Nd content on $\tan\delta$.

The variation of dielectric constant of BFO and $BNFO_x$ ($x = 0.05$, 0.1, 0.15) with frequency at room temperature has been presented in Fig. 3(a). The dielectric constant (ε') for all the samples was found to decreases with increasing frequency, as can be expected from a conventional dielectric relaxation process. The decrease in dielectric constant with increase in frequency is attributed to high values dispersion due to a Maxwell–Wagner type of interfacial polarization, in agreement with Koop's phenomenological theory [25,26]. This is due to the inability of the electric dipoles to be in step with the frequency of the applied electric field. Fig. 3(b) shows the frequency dependence of dielectric loss in BFO and $BNFO_x$ ($x = 0.05$, 0.1, 0.15) ceramics. Similar to the dielectric constant, the dielectric loss also decreases smoothly with increasing frequency. For BFO, low-frequency dispersion in both permittivity and $\tan\delta$ spectra indicates the presence of dc conductivity [27,28]. For $x = 0.05$, 0.1 and 0.15, this low-frequency dispersion and the value of $\tan\delta$ are reduced exhibiting reduced conductivity.

To investigate further the effect of Nd substitution, the dielectric constant and dielectric loss of the BFO and $BNFO_x$ ceramics are re-plotted in inset 2(a) and inset 2(b) respectively as a function of Nd concentration. It is striking to see that the dielectric constant increases dramatically with small amount of Nd substitution (inset 2(a)); for example, the dielectric constant measured at 100 kHz reaches a maximum value of 60 when $x = 0.05$, which is almost twice than that for pure BFO, Further increasing in the Nd content ($x = 0.1$) reduces the value of the dielectric constant back to the level for pure BFO. Another maximum of dielectric constant appears at $x = 0.15$. This dielectric behaviour of $BNFO_x$ ceramics might be understood in terms of oxygen vacancy and the displacement of Fe^{3+} ions. The oxygen vacancies (V_O^{2+}) mainly comes from the Bi volatility and transition from Fe^{2+} to Fe^{3+}, as described in Eqs. (1) and (2):

$$4Bi^{3+} + 6O^{2-} \leftrightarrow 4Bi(gas) + 3O_2(gas) + 4V_{Bi}{}^{3-} + 6V_O{}^{2+} \quad (1)$$

$$4Fe^{3+} + 2O^{2-} \leftrightarrow 4Fe^{2+} + O_2(gas) + 6V_O{}^{2+} \quad (2)$$

The oxygen vacancies are trapping centres for electrons, and the electrons they trapped can be readily activated for conduction by the applied electric filed and thus increase the leakage current density of the ceramics [29]. This significant improvement in dielectric properties can be attributed to the suppression of the formation of impurity and oxygen vacancies by the small amount ($x = 0.05$) Nd^{3+} for volatile Bi^3. Since, the strength of Nd—O bond (703 ± 34 kJ/mol) is higher than that of Bi—O bond (343 ± 6 kJ/mol) [30], the substitution of Nd for Bi in the A site has stabilized the perovskite structure and lowered the concentration of oxygen vacancies.

Further increase in Nd content ($x > 0.05$) would result in a unit cell volume contraction because ionic radius of Nd^{3+} is smaller than that of Bi^{3+}. The free volume available for the displacement of Fe^{3+} ions in the Fe—O oxygen octahedral has become smaller and this would lead to a decrease in dielectric polarization. As Nd content x is greater than 0.1 the mismatch between $BiFeO_3$, and $NdFeO_3$ lattice constant prevents the grains from growing big, which introduces more grain boundaries, which has been also supported by SEM images (Fig. 1). As a result, the dielectric constant has increased again for $BNFO_{0.15}$.

Fig. 4 shows the variation in dielectric constant and dielectric loss (inset) with temperature. Two anomalies around 380 °C and 222 °C were observed for the samples, i.e. $BNFO_{0.05}$ and $BNFO_{0.10}$. Such type of behaviour has also been reported previously by a number of authors [31–36]. Mazumder et al. [36] has observed similar behaviour during their work on particle size dependence of magnetization and phase transition temperature. After in depth analysis of results they concluded that these dielectric anomalies are intrinsic and could not be due to extrinsic factors such as electrode–sample interface or other interfaces such as grain boundaries. The existence of anomaly around 222 °C may be attributed to

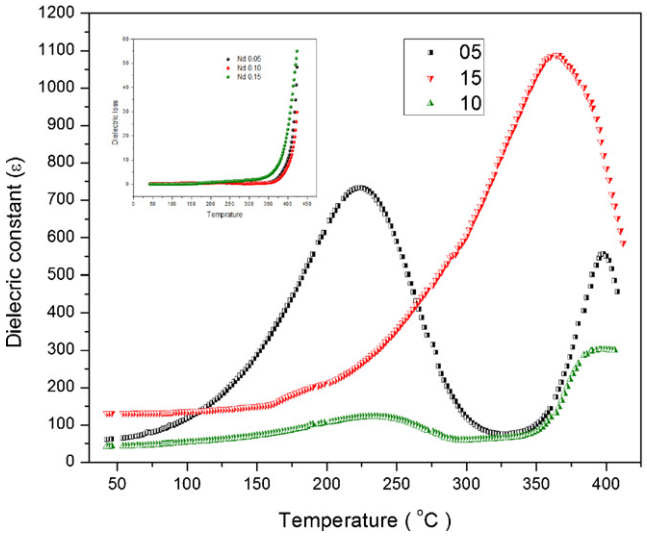

Fig. 4. Temperature dependence of dielectric constants (ε') in $BNFO_x$ samples at 1 MHz and inset represents the variation of dielectric loss with temperature at 1 MHz.

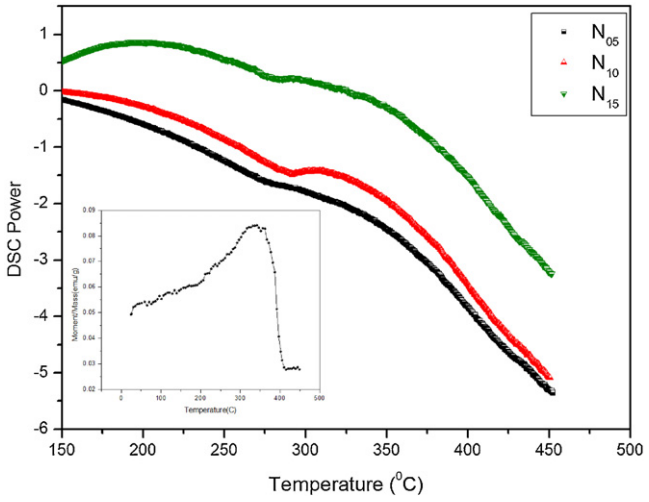

Fig. 5. DSC curve for $BNFO_x$ ($x = 0.05, 0.1, 0.15$) representing AFM to PM transition around 350 °C; inset shows the M–T curve for $x = 0.15$.

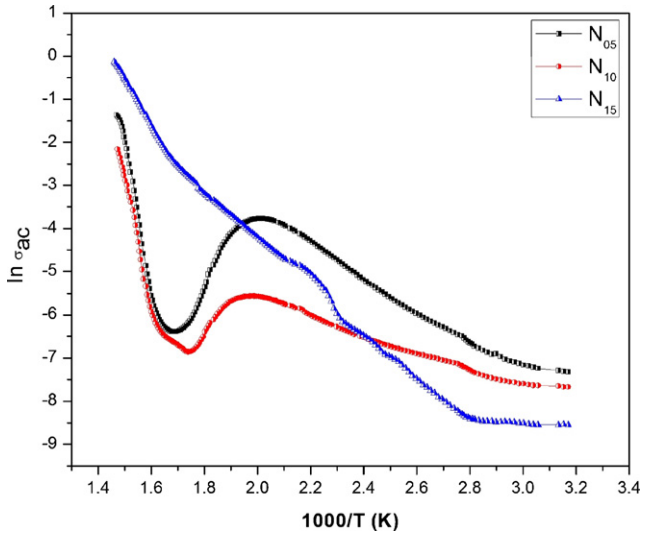

Fig. 6. Variation of ac conductivity ($\ln \sigma_{ac}$) with $1000/T$ of $BNFO_x$ ($x = 0.05, 0.1, 0.15$).

the inhomogeneity and/or oxygen nonstoichiometry arising due to, volatility of Bi near the processing temperature as well as susceptibility of the lattice structure for developing oxygen non-stoichiometry. The Landau–Devonshire theory of phase transitions has predicated such type of dielectric anomaly in magnetoelectrically ordered systems as an effect of vanishing magnetic order on the electric order [36]. The anomaly around 380 °C is observed as a result of magnetic phase transition (T_N) and furthermore, it also confirmed the magneto-electric coupling in the compound. The intensity of anomaly around 222 °C decreased with the substitution and the anomaly at 380 °C is also shifted towards lower temperature region. The single anomaly is observed with $BNFO_{0.15}$, due to the presence of single phase in the sample [16]. The decrease in T_N was further supported by differential scanning calorimetric (DSC) and M–T (magnetic moment as a function of temperature) measurements (Fig. 5). In case of DSC measurement observed anomaly in the curve was due to the vanishing antiferromagnetic ordering in the sample. The magnetic phase transition from antiferro to paramagnetic (PM) was known to be endothermic in nature and responsible for the difference in temperature of crucible with sample and reference. Furthermore, The M–T measurement clearly showed the instant decrease in magnetic moment around 350 °C due to vanishing magnetic order.

Fig. 6 represents the variation of ac conductivity (σ_{ac}) with temperature. The ac conductivity of these samples were calculated using relation $\sigma_{ac} = \varepsilon_0 \omega \varepsilon' \tan\delta$. In the low temperature region, σ_{ac} was relatively small and increased slowly with temperature. In contrast, σ_{ac} increases rapidly with temperature when it is higher than 290 °C. The rapid increase of σ_{ac} with temperature sets a limit for the application of this ceramic. It was observed that, at low temperature region conductivity of the system has decreased with the increase in Nd content, which is quite desirable from the technological point of view.

The temperature dependence of σ_{ac} can be described by the equation: $\sigma_{ac} = \sigma_o \exp(-E_a/k_B T)$, where σ_o is the pre-exponential factor, E_a is the activation energy of ac charge carriers, and k_B is the Boltzmann constant. The E_a values were determined from the slopes of the linear fragments in different temperature region are listed in Table 1. The E_a values for $BNFO_x$ in the region below temperature 493 K is much less than the second ionization energy of oxygen vacancy, which indicates that, the first ionization of oxygen vacancies and electron hopping are responsible for conduction at low temperatures. The value of activation energy at different temperatures for $BNFO_{0.15}$ has showed drastic change from the previous compositions, which can be attributed to the removal of impurity phases and structural change with the Nd substitution. Different amounts of impurity phases and defect ions reveal different oxygen stoichiometries. This further leads to different conductivities depending on the different doping levels. Furthermore, it seems most likely that even up to high temperatures BFO was not dominated by the intrinsic conductivity that would result from the optical gap, but merely by unavoidable impurity contributions and defect centres [37].

Table 1
Value of activation energy in different temperature regions for $BNFO_x$ ($x = 0.05, 0.10$ and 0.15); calculated by using relation $\sigma_{ac} = \sigma_o \exp(-E_a/k_B T)$.

Temperature (K)	Activation energy E_a in eV (approximate values)		
	$N_{0.05}$	$N_{0.10}$	$N_{0.15}$
323	0.198	0.095	0.024
453	0.315	0.239	0.426
670	2.382	2.15	0.934

4. Conclusion

It can be concluded that, the Nd substitution has hindered the formation of secondary phases and oxygen vacancies, which were responsible to deteriorate the multiferroic properties of the BFO compound. The significant improvement in the dielectric as well as the magnetic properties has been observed in doped samples. The anomaly was observed around 380 °C in dielectric constant as a function of temperature because of AFM to PM transition in $BNFO_x$ multiferroic phase and it also confirmed the magneto-electric coupling in the samples. The Néel temperature of the compound has been found to decrease with substitution. Furthermore, Nd substitution has also decreased the ac conductivity, by preventing the generation of the charge carriers.

Acknowledgements

The authors are thankful to University Grant Commission, New Delhi (India) for providing research fellowship (UGC-SAP) and Defence Research Development Organisation (DRDO) for providing grant No. ERIP/ER/0703665/M/01/1044. Research facilities provided by SAIF Chandigarh and NPL New Delhi are highly acknowledged.

References

[1] N.A. Spaldin, Magnetic Materials Fundamentals and Application, 2nd ed., Cambridge University Press, 2010, p. 216.
[2] N.A. Hill, J. Phys. Chem. 104 (2000) 6694–6709.
[3] T. Kimura, G. Lawes, A.P. Ramirez, Phys. Rev. Lett. 94 (2005) 137201–137204.
[4] F. Kubel, H. Schimid, Acta Crystallogr. B 46 (1990) 698–702.
[5] P. Fischer, M. Polomska, I. Sosnowska, M. Szymanski, J. Phys. Solid State Phys. 13 (1980) 1931–1940.
[6] C. Michel, J.-M. Moreau, G.-D. Achenbach, R. Gerson, W.J. James, Solid State Commun. 7 (1969) 701–704.
[7] J. Wang, J.B. Neaton, H. Zheng, V. Nagarajan, S.B. Ogale, B. Liu, D. Viehland, V. Vaithyanathan, D.G. Schlom, U.V. Waghmare, N.A. Spaldin, K.M. Rabe, M. Wuttig, R. Ramesh, Science 299 (2003) 1719–1722.
[8] J. Dho, X. Qi, H. Kim, J.L. MacManus-Driscoll, M.G. Blamire, Adv. Mater. 18 (2006) 1445–1448.
[9] J. Li, J. Wang, M. Wuttig, R. Ramesh, N. Wang, B. Ruette, A.P. Pyatakov, A.K. Zvezdin, D. Viehland, Appl. Phys. Lett. 84 (2004) 5261–5263.
[10] K.Y. Yun, M. Noda, M. Okuyama, H. Saeki, H. Tabata, K. Saito, J. Appl. Phys. 96 (2004) 3399–3403.
[11] K.Y. Yun, M. Noda, M. Okuyama, Appl. Phys. Lett. 83 (2003) 3981–3983.
[12] R.R. Das, D.M. Kim, S.H. Baek, C.B. Eom, F. Zavaliche, S.Y. Yang, R. Ramesh, Y.B. Chen, X.Q. Pan, X. Ke, M.S. Rzchowski, S.K. Streiffer, Appl. Phys. Lett. 88 (2006) 242904–242906.
[13] C. Ederer, N.A. Spaldin, Phys. Rev. B 71 (R) (2005) 060401–060404.
[14] J.B. Neaton, C. Ederer, U.V. Waghmare, N.A. Spaldin, K.M. Rabe, Phys. Rev. B 71 (2005) 014113–014120.
[15] K. Sen, S. Thakur, K. Singh, A. Gautam, M. Singh, Mater. Lett. 65 (2011) 1963–1965.
[16] A. Gautam, K. Singh, K. Sen, R.K. Kotnala, M. Singh, Mater. Lett. 65 (2011) 591–594.
[17] G.D. Hu, S.H. Fan, C.H. Yang, W.B. Wu, Appl. Phys. Lett. 92 (2008) 192905–192907.
[18] V.R. Reddy, D. Kothari, A. Gupta, S.M. Gupta, Appl. Phys. Lett. 94 (2009) 082505–082507.
[19] D.H. Wang, W.C. Goh, M. Ning, C.K. Ong, Appl. Phys. Lett. 88 (2006) 212907–212909.
[20] V.A. Khomchenko, D.A. Kiselev, J.M. Vieira, L. Jian, A.L. Kholkin, A.M.L. Lopes, Y.G. Pogorelov, J.P. Araujo, M. Maglione, J. Appl. Phys. 103 (2008) 024105–024110.
[21] M. Kumar, K.L. Yadav, J. Phys. Condens. Matter 18 (2006) L503.
[22] F.G. Chang, N. Zhang, F. Yang, S.X. Wang, G.L. Song, J. Phys. D: Appl. Phys. 40 (2007) 7799.
[23] M. Kumar, K.L. Yadav, J. Appl. Phys. 100 (2006) 074111–074114.
[24] M. Azuma, H. Kanda, A.A. Belik, Y. Shimakawa, M. Takano, J. Magn. Magn. Mater. 310 (2007) 1177.
[25] J.C. Maxwell, Electricity and Magnetism, vol. 1, Section 328, Oxford University Press, London, 1873.
[26] C.G. Koops, Phys. Rev. 83 (1951) 121–124.
[27] A.K. Jonscher, Nature 267 (1977) 673–679.
[28] A.K. Jonscher, F. Meca, H.M. Millany, C. Phys, Solid State Phys. 12 (1979) L293.
[29] V.R. Palkar, Appl. Phys. Lett. 80 (2002) 1628–1630.
[30] J.A. Dean, Lange's Handbook of Chemistry, 15th ed., McGraw-Hill, New York, 1999.
[31] S. Karimi, I.M. Reaney, I. Levin, I. Sterianou, Appl. Phys. Lett. 94 (2009) 112903–112905.
[32] P. Uniyal, K.L. Yadav, J. Phys. Condens. Matter 21 (2009) 405901.
[33] W.M. Zhu, Z.-G. Ye, Ceram. Int. 30 (2004) 1435–1442.
[34] N.N. Krainik, N.P. Khuchua, V.V. Zhdanova, V.A. Evseev, Sov. Phys. Solid State 8 (3) (1966) 654.
[35] J. Wang, J.B. Neaton, H. Zheng, V. Nagarajan, S.B. Ogale, B. Liu, D. Viehland, V. Vaithyanathan, D.G. Schlom, U.V. Waghmare, N.A. Spaldin, K.M. Rabe, M. Wuttig, R. Ramesh, Science 299 (2003) 1719–1722.
[36] R. Mazumder, S. Ghosh, P. Mondal, D. Bhattacharya, S. Dasgupta, N. Das, A. Sen, A.K. Tyagi, M. Sivakumar, T. Takami, H. Ikuta, J. Appl. Phys. 100 (2006) 33908–033916.
[37] J. Lu, A. G¨unther, F. Schrettle, F. Mayr, S. Krohns, P. Lunkenheimer, A. Pimenov, V.D. Travkin, A.A. Mukhin, A. Loidl, Eur. Phys. J. B 75 (2010) 451–460.